

Z' signals in polarised top-antitop final states

L. Basso¹, K. Mimasu², S. Moretti^{2,3}

¹Physikalisches Institut, Albert-Ludwigs-Universität Freiburg, Germany

²School of Physics & Astronomy, University of Southampton, UK

³Particle Physics Department, Rutherford Appleton Laboratory, UK

[arXiv:1203.2542](https://arxiv.org/abs/1203.2542)



UNIVERSITY OF
Southampton

Overview

- Introduction
 - Extra neutral gauge bosons
 - $t\bar{t}$ channel: Asymmetries at the LHC
- Benchmark Z' models and asymmetries
- Our study
- Results
 - Differential distributions
 - Significance and luminosity analysis
- Summary & outlook

Introduction

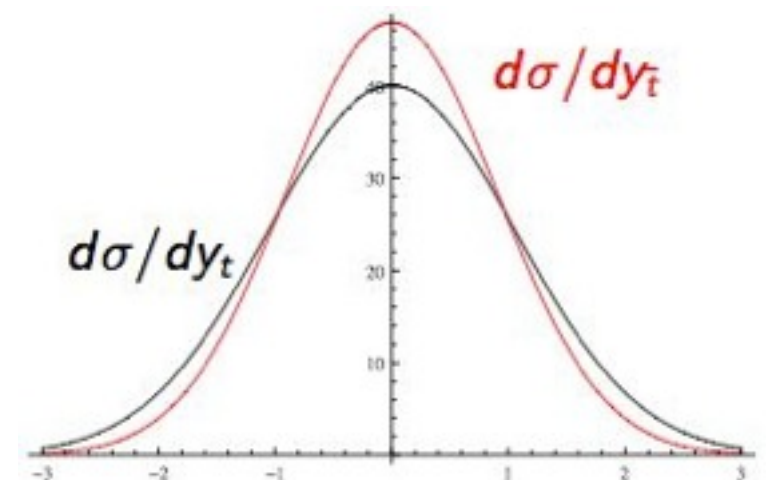
- Z' : massive neutral s-channel resonance
 - Extra gauge boson from an extension of the SM symmetry group
 - KK excitation of SM gauge fields in extra dimensions
 - Spin-2 graviton
 - Many more...
- Drell-Yan: $pp(p\bar{p}) \rightarrow Z' \rightarrow l^+l^-$
 - Discovery channel
 - Low background $\sim 100\%$ reconstruction efficiency
- $Z' \rightarrow t\bar{t}$ also has a role to play being another significant channel at the LHC

$t\bar{t}$ channel

- Mass near the EW scale
 - Strongly coupled to EWSB dynamics, Important component of BSM theories
- Large production cross section at the LHC
 - BSM searches: irreducible QCD ‘background’
 - More involved 6 body final state
 - Lower reconstruction efficiency $\sim 10\%$
- Theoretical cross sections well known (NNLO)
- Z' : access to up-type quark couplings
- Top quark decays before hadronisation
 - Charge, spin information propagated to decay products

Asymmetries

- Charge (spatial) asymmetry
 - Measure of the symmetry of a process under charge conjugation ($q\bar{q} \rightarrow f^+f^-$)
 - CP invariance \rightarrow symmetry of angular dependence of matrix element (θ : angle between incoming quark and outgoing top)
- Tevatron: $t\bar{t}$ forward backward asymmetry A_{FB}
- LHC: symmetric pp collider
 - Cannot define an absolute ‘forward’ direction
 - Boost of CM frame correlated with incoming quark direction
 - Top rapidity distribution broadened w.r.t antitop

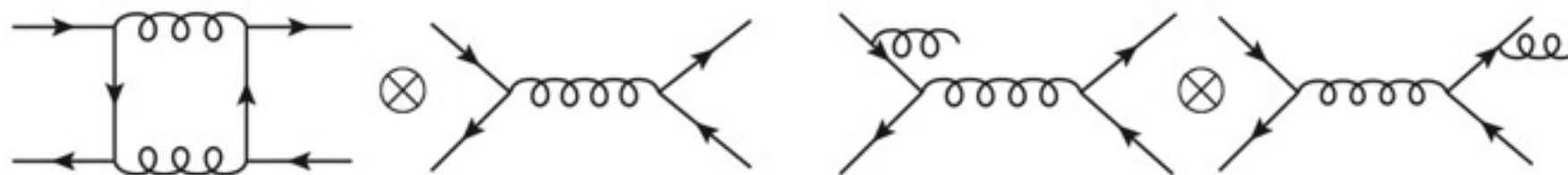


Charge asymmetry

- Dominant SM contribution: $O(\alpha^3)$ QCD

[Halzen '87; Kuhn, Rodrigo '99]

- gg is C-symmetric
- Interference of ISR and FSR
- Box diagram with tree level



- Define variables accordingly:

- Restrict rapidity range and compare tops vs. antitops
- Rapidity difference + kinematical cuts to enhance qqbar

[Zhou et al. '11]

$$A_C = \frac{N_t(|y| < y_{cut}^C) - N_{\bar{t}}(|y| < y_{cut}^C)}{N_t(|y| < y_{cut}^C) + N_{\bar{t}}(|y| < y_{cut}^C)}$$

$$A_F = \frac{N_t(|y| > y_{cut}^F) - N_{\bar{t}}(|y| > y_{cut}^F)}{N_t(|y| > y_{cut}^F) + N_{\bar{t}}(|y| > y_{cut}^F)}$$

$$A_{OFB} = \frac{N(\Delta y > 0) - N(\Delta y < 0)}{N(\Delta y > 0) + N(\Delta y < 0)} \bigg|_{|p_{t\bar{t}}^z| > p_{cut}^z}$$

$$A_{RFB} = \frac{N(\Delta y > 0) - N(\Delta y < 0)}{N(\Delta y > 0) + N(\Delta y < 0)} \bigg|_{|y_{t\bar{t}}| > |y_{t\bar{t}}^{cut}|}$$

Spin asymmetry

- Defined in terms of the helicity of the outgoing top/antitop
- Single (L) and double (LL) spin asymmetries
 - Can be extracted from kinematical properties of top decay products

$$A_{LL} = \frac{N(+, +) + N(-, -) - N(+, -) - N(-, +)}{N_{Total}}$$
$$A_L = \frac{N(-, -) + N(-, +) - N(+, +) - N(+, -)}{N_{Total}}$$

- $N(h_t, h_{tbar})$ obtained by calculating unpolarised matrix elements using helicity amplitude methods
[Hagiwara, Zeppenfeld '85 ; Mangano, Parke '90; Arai et al. '08]
- Asymmetries are and independent probe of Chiral couplings of new physics to tops

Z': Model definitions

- Study based on set of benchmark models defined in *[Accomando, Belyaev, Fedeli, King, Shepherd-Themistocleous. arXiv:1010.6058]*
- TeV scale extra U(1):
 - Universal couplings to generations
 - Fields in the same SM representations will have the same charge under new U(1)
 - → 5 independent couplings Q_L, L_L, u_R, d_R, e_R (ν_R decoupled)
- Parametrise generic Z' interaction in vector-axial basis:

$$\mathcal{L}_{Z'} = \frac{g'}{2} Z'_\mu \bar{\psi}^i \gamma^\mu (g_V^i + g_A^i \gamma^5) \psi^i$$

Z': Models

- E_6 models

- Two additional $U(1)$'s from GUT group breaking pattern
- $E_6 \rightarrow SO(10) \otimes U(1)_\psi \rightarrow SU(5) \otimes U(1)_\psi \otimes U(1)_\chi \rightarrow SM \otimes U(1)_\psi \otimes U(1)_\chi$
- Linear combination survives down to TeV scale
- $Q(E_6) = \cos\theta T_\chi + \sin\theta T_\psi$

- Left-Right symmetric

- $SU(2)_L \otimes SU(2)_R \otimes U(1)_{B-L} \rightarrow SU(2)_L \otimes U(1)_Y$
- $U(1)_R \otimes U(1)_{B-L} \rightarrow U(1)_Y$
- $Q(G_{LR}) = \cos\phi T_{3R} + \sin\phi T_{B-L}$

- Generalised sequential SM

- Sequential = SM couplings : Standard candle in experimental searches
- $Q(G_{SM}) = \cos\alpha T_{3L} + \sin\alpha Q_{EM}$

Z': Couplings

$U(1)'$	Parameter	g_V^u	g_A^u	g_V^d	g_A^d
<hr/>					
E_6 ($g' = 0.462$)	θ				
$U(1)_\chi$	0	0	-0.316	-0.632	0.316
$U(1)_\psi$	0.5π	0	0.408	0	0.408
$U(1)_\eta$	-0.29π	0	-0.516	-0.387	-0.129
$U(1)_S$	0.129π	0	-0.129	-0.581	0.452
$U(1)_N$	0.42π	0	0.316	-0.158	0.474
<hr/>					
G_{LR} ($g' = 0.595$)	ϕ				
$U(1)_R$	0	0.5	-0.5	-0.5	0.5
$U(1)_{B-L}$	0.5π	0.333	0	0.333	0
$U(1)_{LR}$	-0.128π	0.329	-0.46	-0.591	0.46
$U(1)_Y$	0.25π	0.589	-0.354	-0.118	0.354
<hr/>					
G_{SM} ($g' = 0.760$)	α				
$U(1)_{SM}$	-0.072π	0.193	0.5	-0.347	-0.5
$U(1)_{T_{3L}}$	0	0.5	0.5	-0.5	-0.5
$U(1)_Q$	0.5π	1.333	0	-0.666	0
<hr/>					

- Study of asymmetry variables in $t\bar{t}b\bar{b}$ from broad classes of Z' models being searched for at the LHC
 - Sensitivity to chiral couplings to up quarks
 - Distinguishability from SM and amongst themselves

Z': asymmetries

- Charge asymmetry

- Asymmetric part of the matrix element ($\cos \theta$ term) proportional to $g_V^i g_A^i g_V^t g_A^t$
- Requires all non-zero couplings to generate at tree-level
- Purely vector/axial models only generate via interference with SM

- Spin asymmetries

- Calculated using helicity amplitudes
- A_{LL} depends in square of top couplings like σ_{total}
- A_L only non-zero if both $g_V^t g_A^t$ non-zero, sensitive to relative sign in these couplings

$$A_{LL}^i \propto \left(3 (g_A^t)^2 \beta^2 + (g_V^t)^2 (2 + \beta^2) \right) \left((g_V^i)^2 + (g_A^i)^2 \right)$$

$$A_L^i \propto g_A^t g_V^t \beta \left((g_V^i)^2 + (g_A^i)^2 \right); \quad \beta = \sqrt{1 - \frac{4m_t^2}{\hat{s}}}$$

Phenomenological study

Abstract

We study the sensitivity of top-antitop samples produced at all energy stages of the Large Hadron Collider (LHC) to the nature of an underlying Z' boson, in presence of full tree level standard model (SM) background effects and relative interferences. We concentrate on differential mass spectra as well as both spatial and spin asymmetries thereby demonstrating that exploiting combinations of these observables will enable one to distinguish between sequential Z' 's and those pertaining to Left-Right symmetric models as well as E_6 inspired ones, assuming realistic final state reconstruction efficiencies and error estimates.

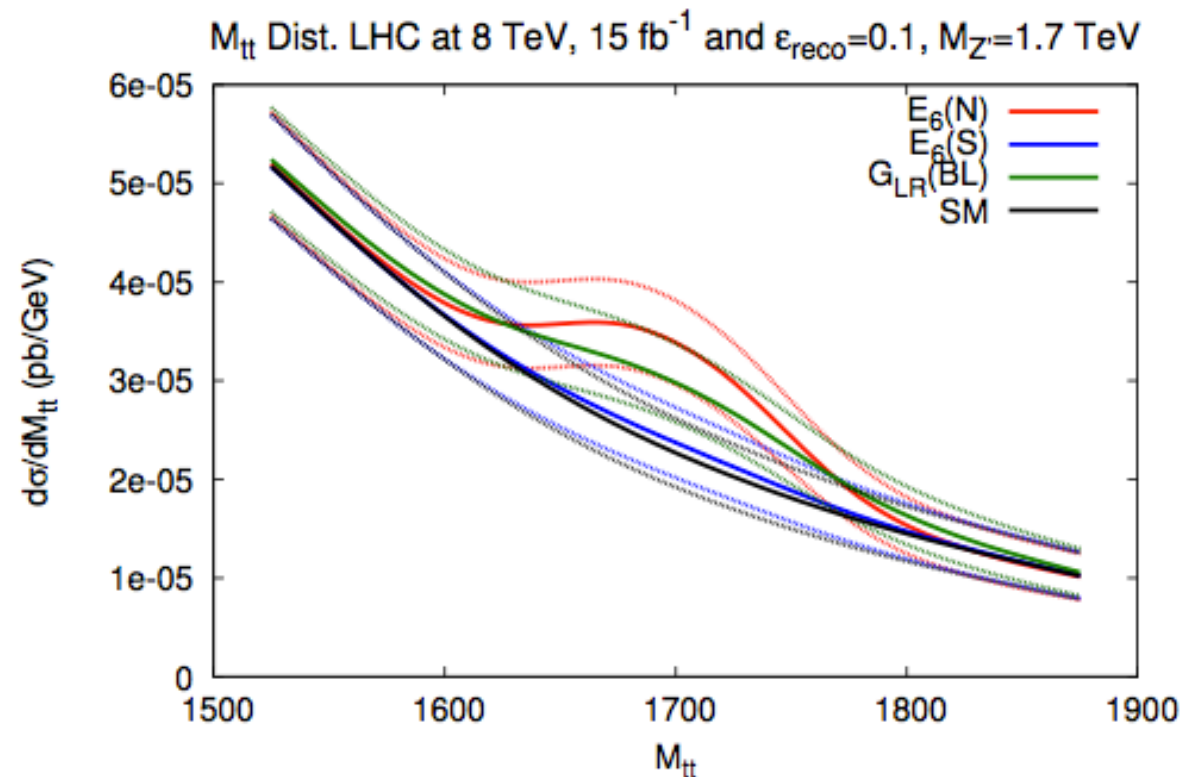
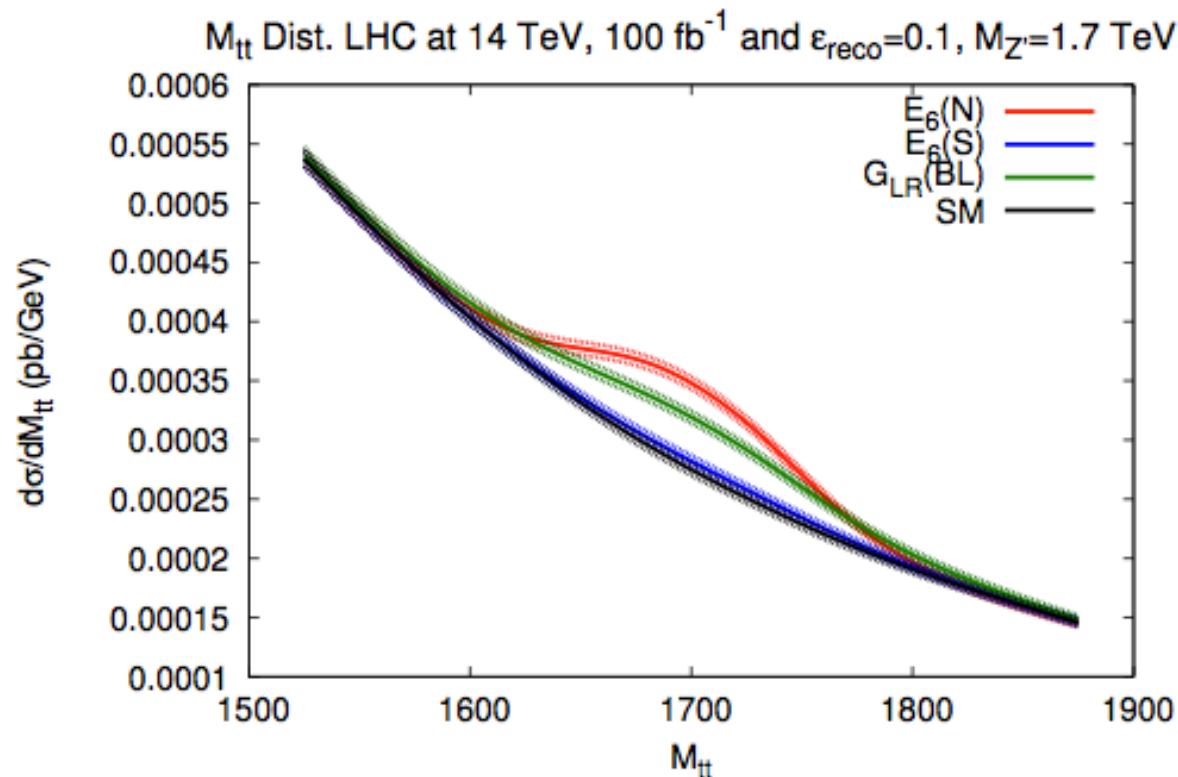
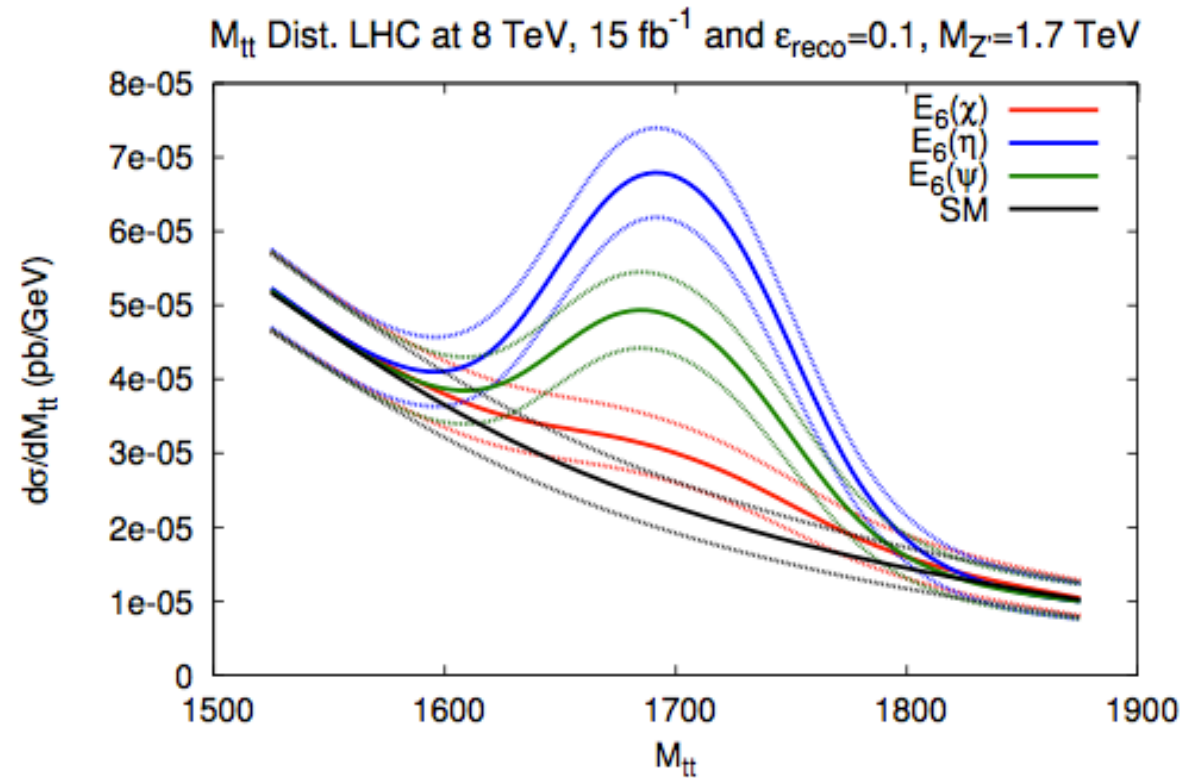
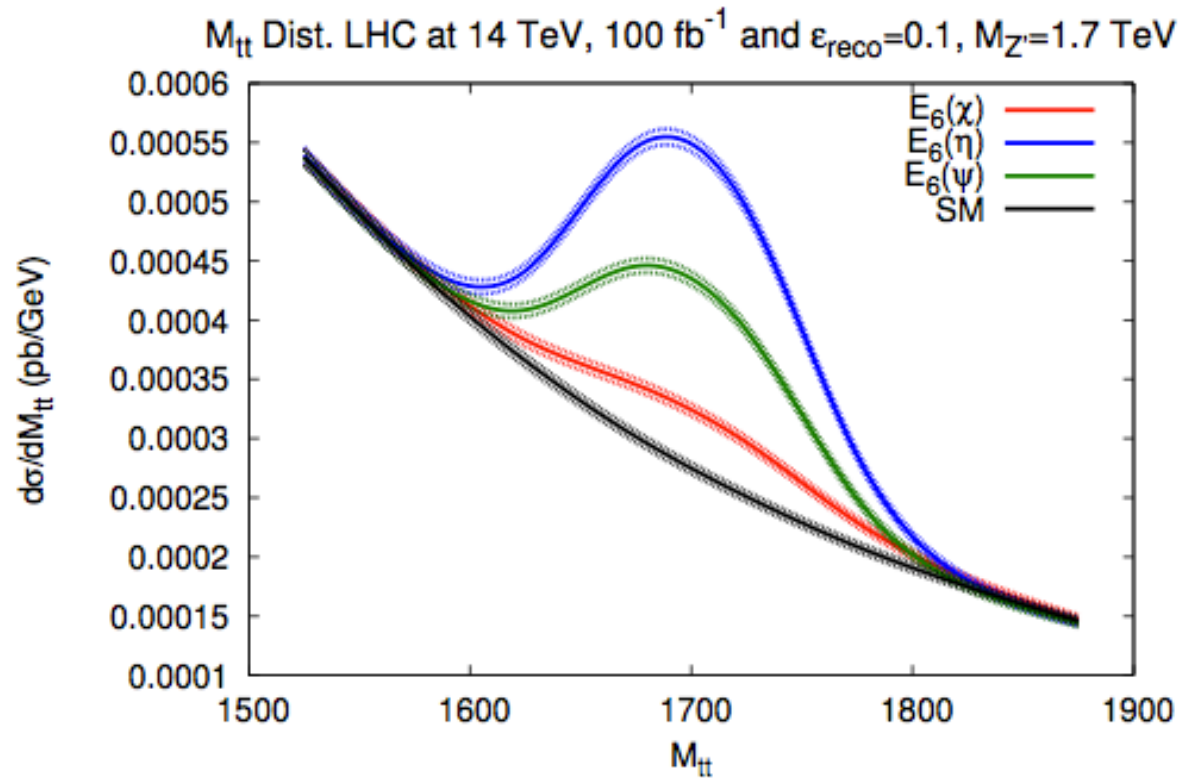
- Developed a tool based on HELAS/MADGRAPH that can output observables in $t\bar{t}$ final state
- Generated invariant mass distributions, invariant mass profiles of asymmetries at parton level for Z' models with tree-level SM and interference
- Split models into two classes
 - ‘ E_6 type’: $E_6 + G_{LR}(B-L)$ - only one non-zero up-type coupling
 - ‘Generalised’: $G_{LR} + G_{SM}$ - both non-zero
- Focus around Z' peak: $|M_{t\bar{t}} - M_{Z'}| < 500 \text{ GeV}$

Details

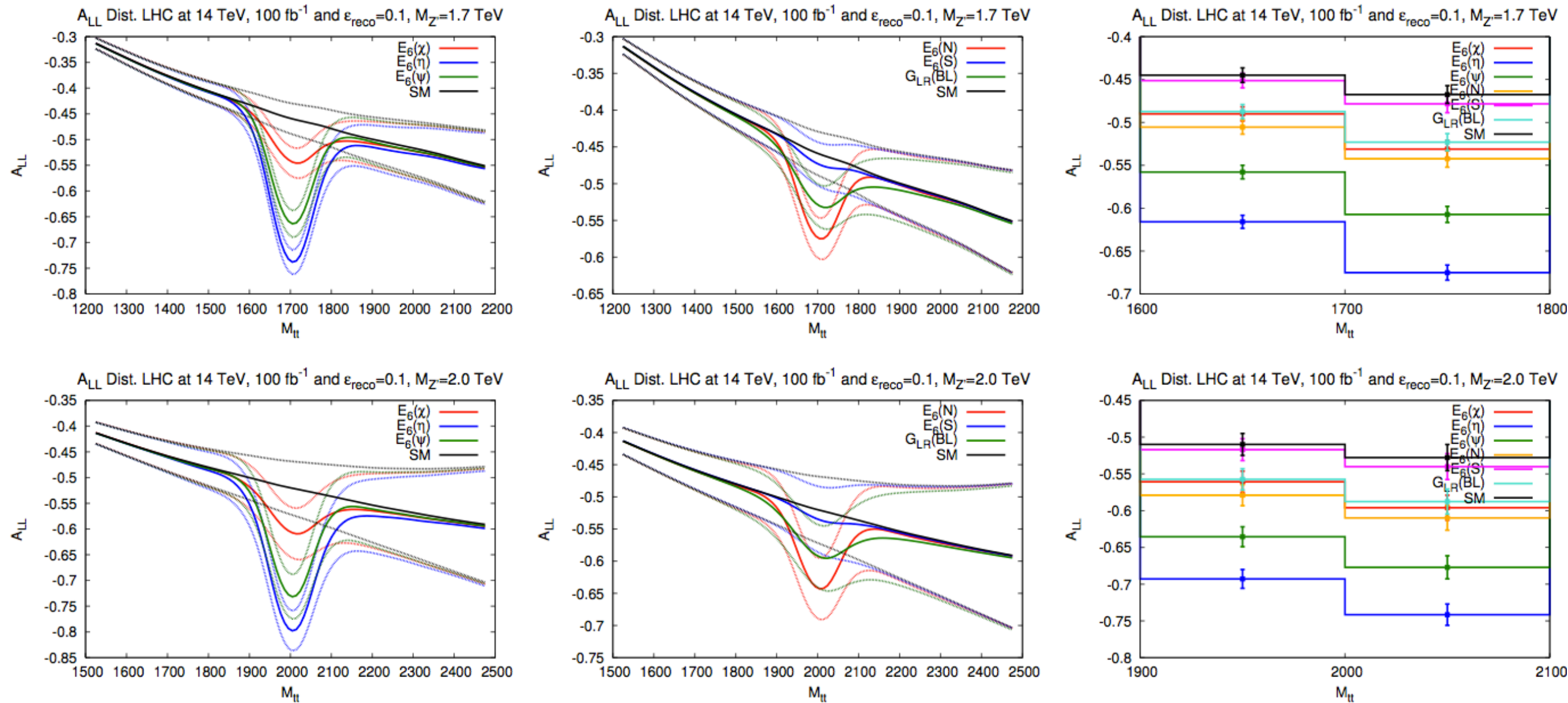
- Numerical code:
 - Took top mass of 175 GeV, all other quarks massless
 - CTEQ6L1 PDF set with $Q=2m_t$
 - VEGAS for numerical integration
 - Simulated LHC at 7, 8, 14 TeV assuming $L_{\text{int}} = (5, 15, 100 \text{ fb}^{-1})$
 - $M_{Z'}=1.7$ and 2 TeV
 - Folded in ttbar reconstruction efficiency $\varepsilon=10\%$
- Statistical error on generic asymmetry δA
 - Based on invariant mass bins of 50 GeV
- ‘Significance’ measure s of distinguishability between models

$$\delta A \equiv \delta \left(\frac{N_F - N_B}{N_F + N_B} \right) = \sqrt{\frac{2}{\mathcal{L}\varepsilon} \left(\frac{\sigma_F^2 + \sigma_B^2}{\sigma_{\text{Total}}^3} \right)} \quad s \equiv \frac{|A(1) - A(2)|}{\sqrt{\delta A(1)^2 + \delta A(2)^2}}$$

Results: E_6 type models



E₆ type models: A_{LL}



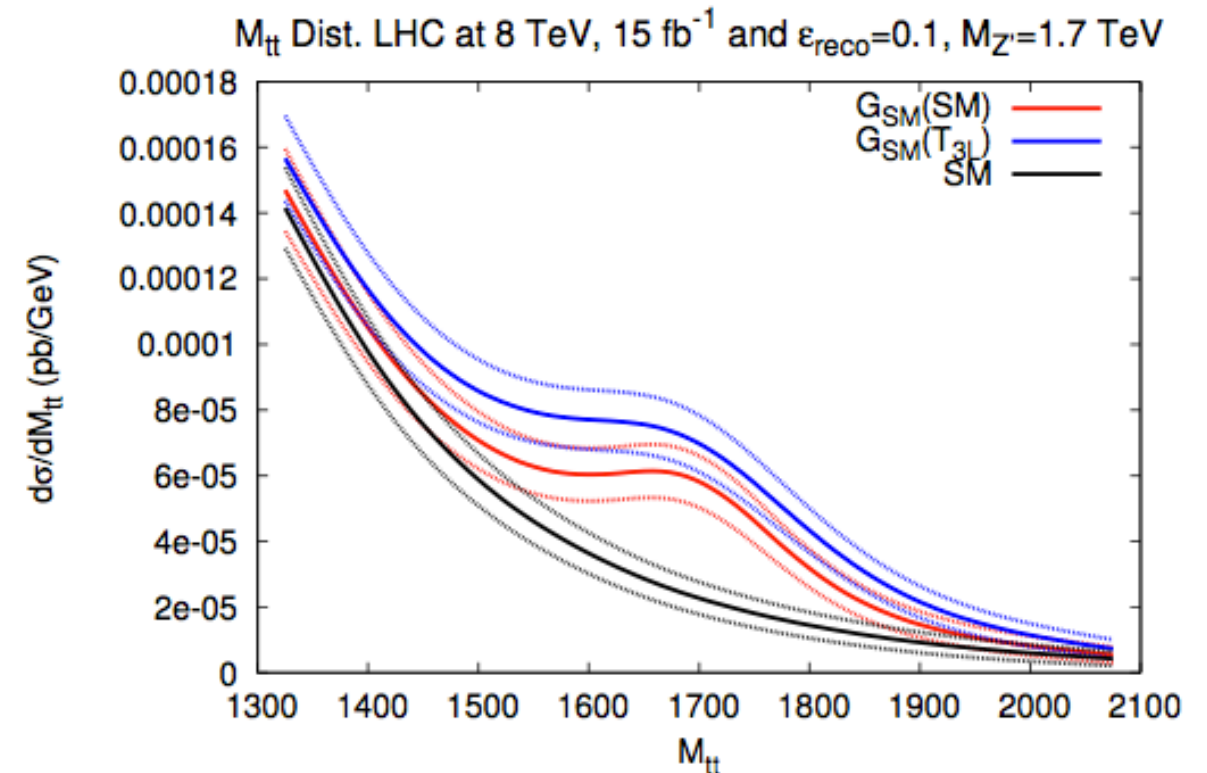
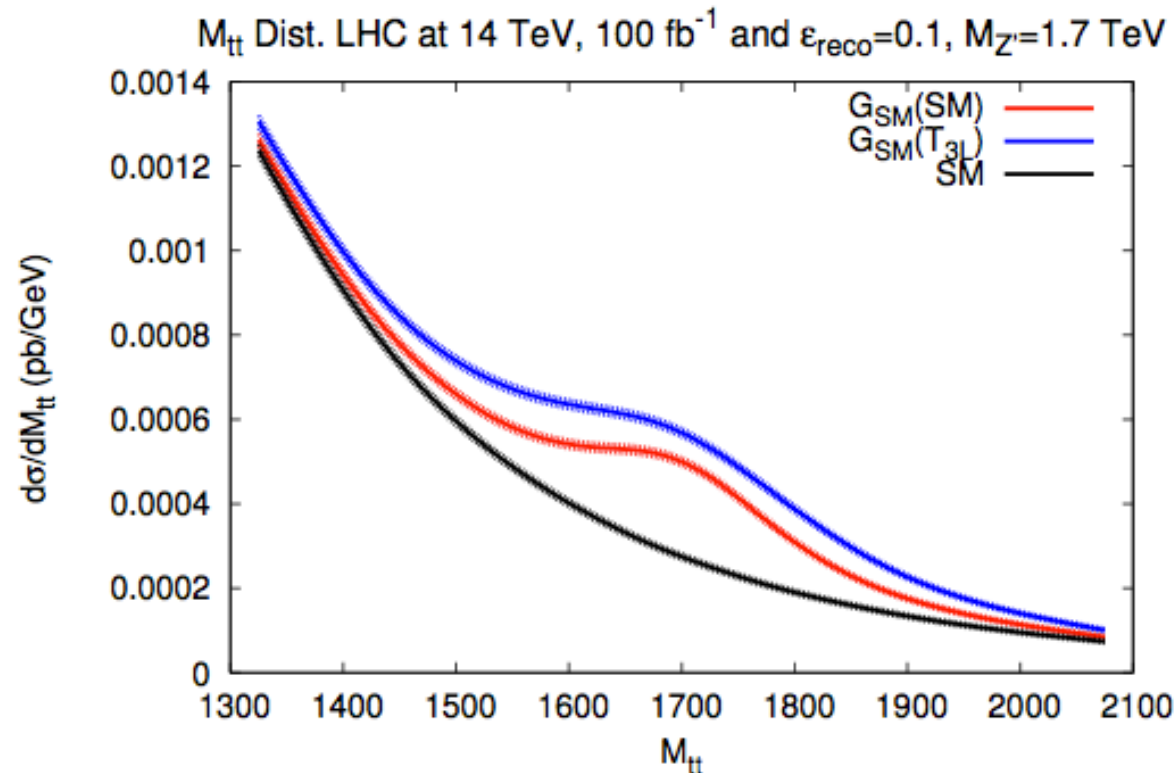
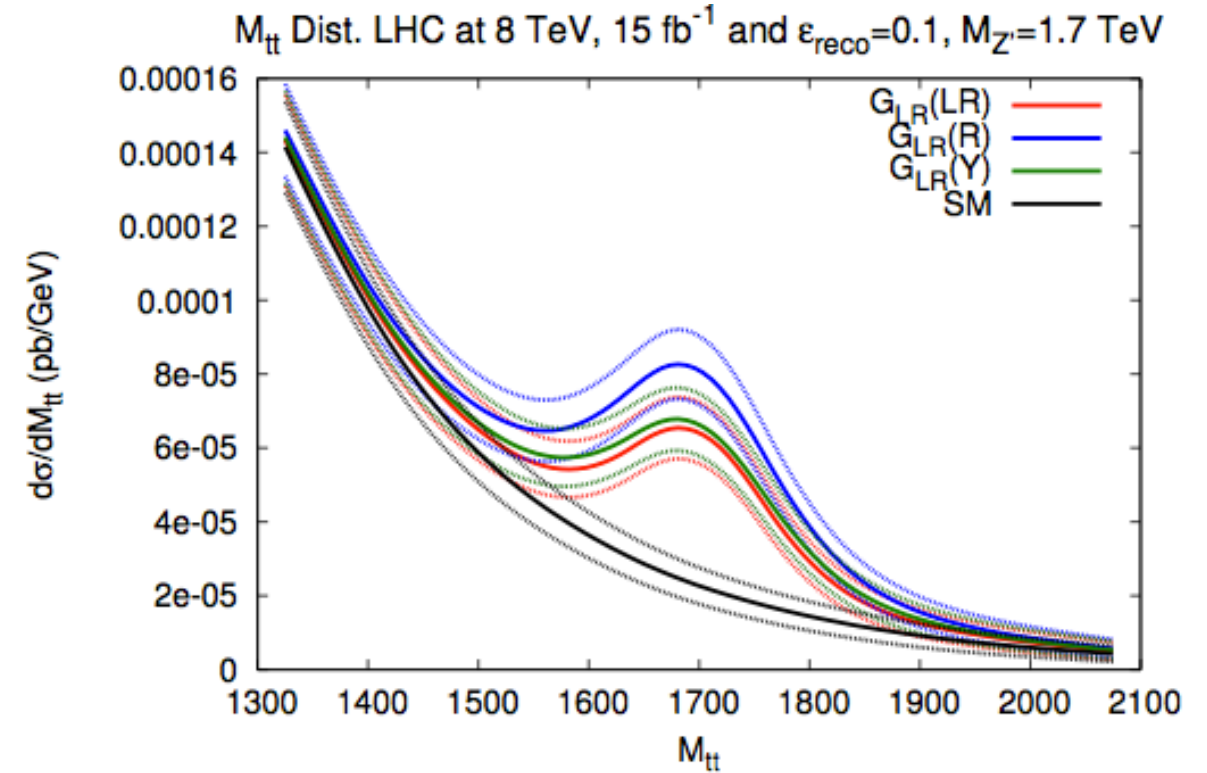
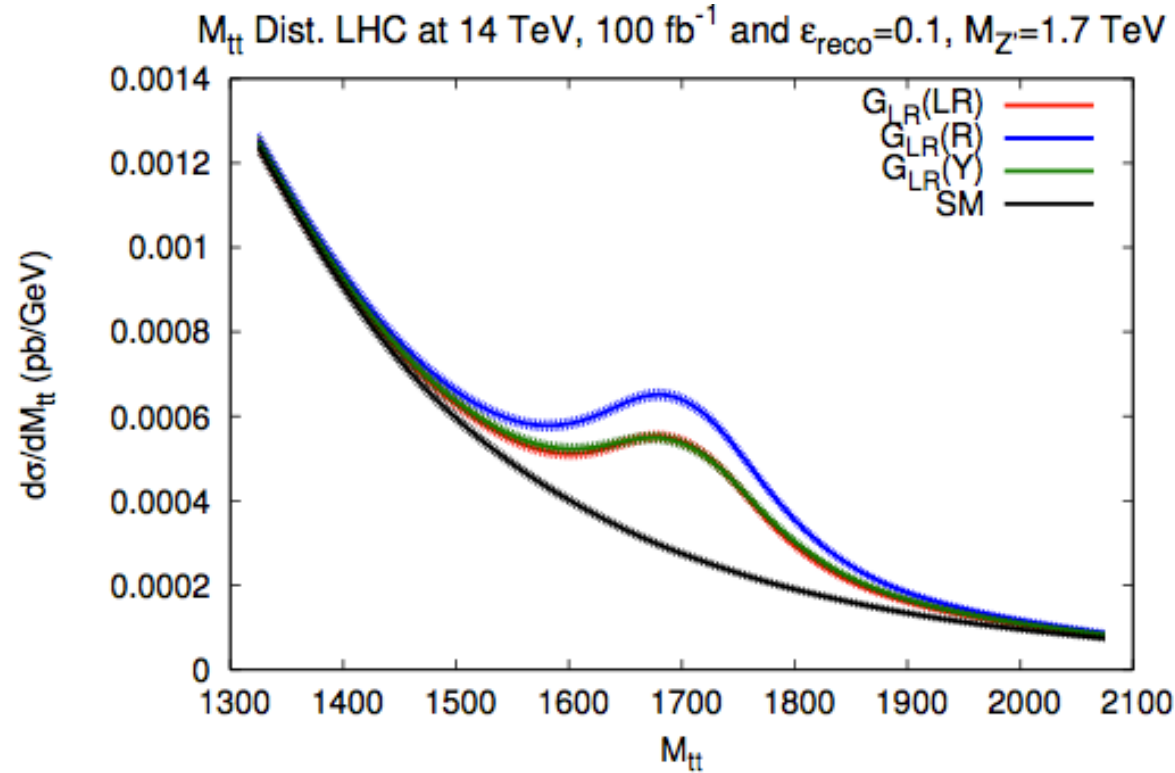
- Clear signatures with distinction between most models and the SM when up-type coupling is large enough
- Set of overlapping models have similar magnitude v/a couplings
- Neither A_{LL} nor cross section measurements can distinguish these

E₆ type models: A_{LL}

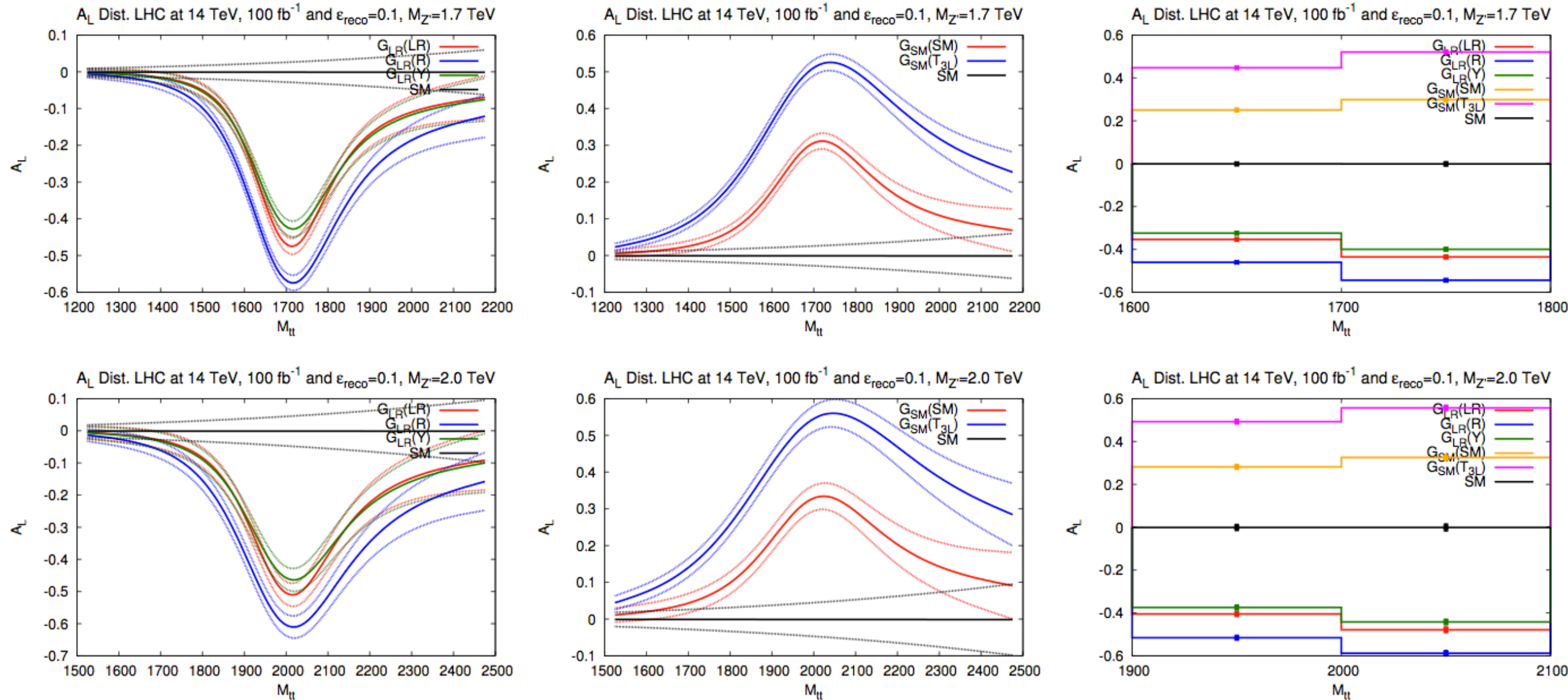
- Integrating over narrow mass window around the peak increases significances

$A_{LL}(\times 10)$	$\sqrt{s} = 14 \text{ TeV}$	$\mathcal{L}_{int} = 100 \text{ fb}^{-1}$	$\sqrt{s} = 8 \text{ TeV}$	$\mathcal{L}_{int} = 15 \text{ fb}^{-1}$
$M_{Z'} = 1.7 \text{ TeV}$	$\Delta M_{t\bar{t}} < 0.5 \text{ TeV}$	$\Delta M_{t\bar{t}} < 0.1 \text{ TeV}$	$\Delta M_{t\bar{t}} < 0.5 \text{ TeV}$	$\Delta M_{t\bar{t}} < 0.1 \text{ TeV}$
SM	-3.79 ± 0.05	-4.54 ± 0.07	-4.75 ± 0.39	-5.65 ± 0.61
$E_6(\chi)$	-3.88 ± 0.05	-5.07 ± 0.06	-4.85 ± 0.39	-6.35 ± 0.58
$E_6(\eta)$	-4.17 ± 0.05	-6.42 ± 0.06	-5.22 ± 0.38	-7.85 ± 0.48
$E_6(\psi)$	-4.01 ± 0.05	-5.79 ± 0.06	-5.02 ± 0.33	-7.22 ± 0.52
$E_6(N)$	-3.90 ± 0.05	-5.21 ± 0.06	-4.88 ± 0.39	-6.54 ± 0.57
$E_6(S)$	-3.80 ± 0.05	-4.62 ± 0.07	-4.76 ± 0.39	-5.76 ± 0.61
$G_{LR}(B - L)$	-3.88 ± 0.05	-5.02 ± 0.06	-4.86 ± 0.39	-6.31 ± 0.57
$M_{Z'} = 2.0 \text{ TeV}$	$\Delta M_{t\bar{t}} < 0.5 \text{ TeV}$	$\Delta M_{t\bar{t}} < 0.1 \text{ TeV}$	$\Delta M_{t\bar{t}} < 0.5 \text{ TeV}$	$\Delta M_{t\bar{t}} < 0.1 \text{ TeV}$
SM	-4.66 ± 0.09	-5.17 ± 0.11	-5.68 ± 0.84	-6.32 ± 1.23
$E_6(\chi)$	-4.77 ± 0.09	-5.76 ± 0.11	-5.81 ± 0.83	-7.03 ± 1.14
$E_6(\eta)$	-5.13 ± 0.09	-7.15 ± 0.10	-6.26 ± 0.80	-8.44 ± 0.89
$E_6(\psi)$	-4.94 ± 0.09	-6.54 ± 0.10	-6.02 ± 0.82	-7.90 ± 1.00
$E_6(N)$	-4.79 ± 0.09	-5.92 ± 0.11	-5.84 ± 0.83	-7.23 ± 1.11
$E_6(S)$	-4.67 ± 0.09	-5.27 ± 0.11	-5.70 ± 0.84	-6.43 ± 1.22
$G_{LR}(B - L)$	-4.77 ± 0.09	-5.70 ± 0.11	-5.82 ± 0.83	-7.00 ± 1.13

Results: Generalised models



Generalised models: A_L



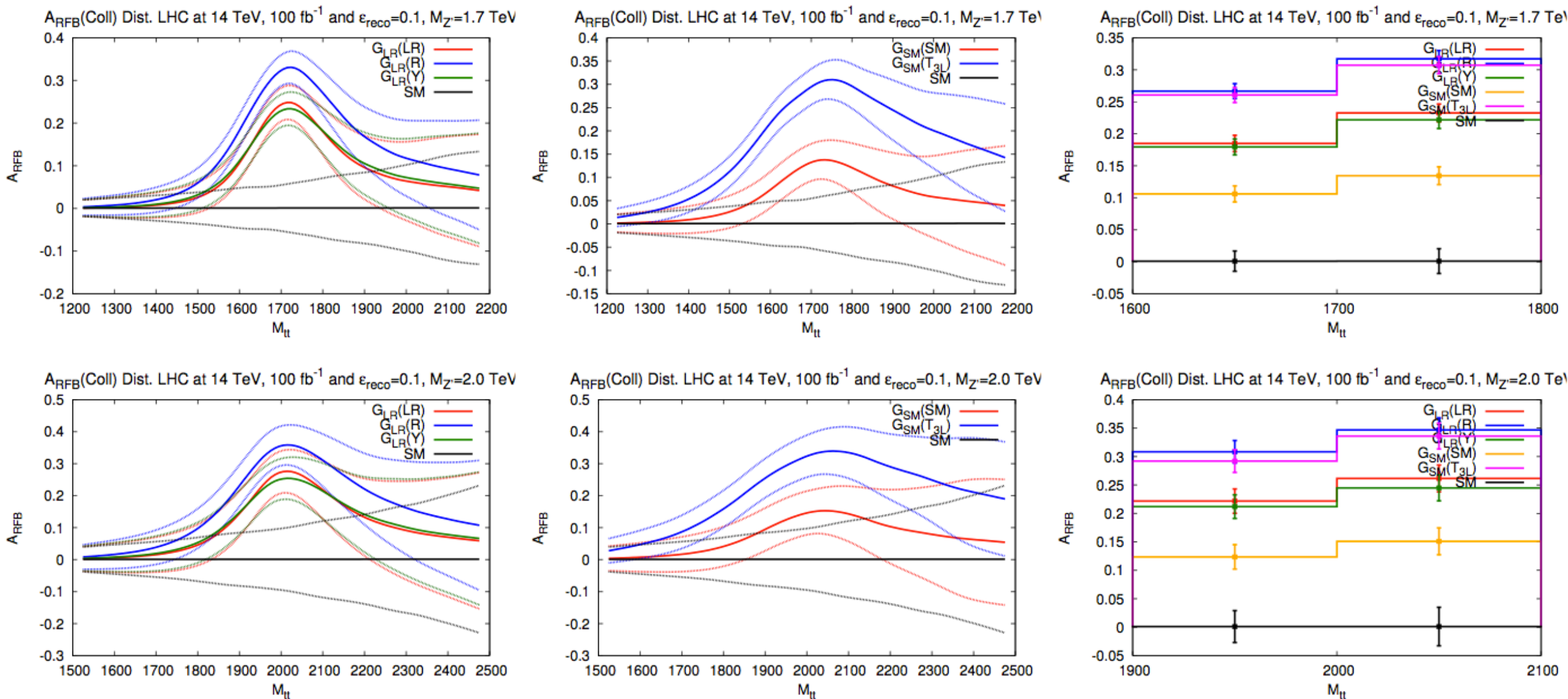
- Larger couplings contribute to more visible effects, increased width
- Good discrimination among models, sensitivity to relative sign of vector and axial couplings: G_{LR} and G_{SM} can be separated

Generalised models: A_L

- $G_{LR}(LR)$ and $G_{LR}(Y)$ are not visibly distinguishable in the invariant mass distributions due to similar magnitude of couplings but can be disentangled by the narrow mass window

$A_L(\times 10)$	$\sqrt{s} = 14 \text{ TeV}$	$\mathcal{L}_{int} = 100 \text{ fb}^{-1}$	$\sqrt{s} = 8 \text{ TeV}$	$\mathcal{L}_{int} = 15 \text{ fb}^{-1}$
$M_{Z'} = 1.7 \text{ TeV}$	$\Delta M_{t\bar{t}} < 0.5 \text{ TeV}$	$\Delta M_{t\bar{t}} < 0.1 \text{ TeV}$	$\Delta M_{t\bar{t}} < 0.5 \text{ TeV}$	$\Delta M_{t\bar{t}} < 0.1 \text{ TeV}$
SM	-0.009 ± 0.044	-0.010 ± 0.059	-0.017 ± 0.35	-0.020 ± 0.53
$G_{LR}(LR)$	-0.971 ± 0.042	-3.90 ± 0.05	-1.37 ± 0.33	-5.36 ± 0.40
$G_{LR}(R)$	-1.51 ± 0.04	-4.98 ± 0.05	-2.14 ± 0.32	-6.53 ± 0.37
$G_{LR}(Y)$	-0.938 ± 0.042	-3.58 ± 0.05	-1.40 ± 0.33	-5.05 ± 0.38
$G_{SM}(SM)$	0.802 ± 0.042	2.71 ± 0.05	1.16 ± 0.32	3.79 ± 0.38
$G_{SM}(T_{3L})$	1.90 ± 0.04	4.80 ± 0.05	2.70 ± 0.31	6.36 ± 0.38
$M_{Z'} = 2.0 \text{ TeV}$	$\Delta M_{t\bar{t}} < 0.5 \text{ TeV}$	$\Delta M_{t\bar{t}} < 0.1 \text{ TeV}$	$\Delta M_{t\bar{t}} < 0.5 \text{ TeV}$	$\Delta M_{t\bar{t}} < 0.1 \text{ TeV}$
SM	-0.011 ± 0.088	-0.012 ± 0.10	-0.020 ± 0.73	-0.020 ± 1.04
$G_{LR}(LR)$	-1.38 ± 0.07	-4.38 ± 0.08	-1.91 ± 0.66	-5.81 ± 0.75
$G_{LR}(R)$	-2.09 ± 0.07	-5.49 ± 0.08	-2.91 ± 0.64	-6.97 ± 0.69
$G_{LR}(Y)$	-1.34 ± 0.07	-4.05 ± 0.08	-1.99 ± 0.65	-5.54 ± 0.71
$G_{SM}(SM)$	1.12 ± 0.07	3.01 ± 0.08	1.59 ± 0.65	4.07 ± 0.71
$G_{SM}(T_{3L})$	2.55 ± 0.07	5.21 ± 0.08	3.53 ± 0.62	6.74 ± 0.71

Generalised models: A_{RFB}



- Performed best among charge asymmetries
- Clearly visible above SM

Significance

- Significance s of A_L and A_{RFB} between models, $M_Z=1.7[2]$ TeV in upper[lower] triangles, invariant mass window $\Delta M=100(500)$ GeV, LHC at 14 TeV $L=100\text{fb}^{-1}$

A_L	SM	$G_{LR}(LR)$	$G_{LR}(R)$	$G_{LR}(Y)$	$G_{SM}(SM)$	$G_{SM}(T_{3L})$
SM	—	50.0(22.8)	63.9(37.3)	45.9(22.0)	35.0(19.2)	61.8(47.4)
$G_{LR}(LR)$	34.1(12.2)	—	15.3(9.3)	4.5(0.6)	93.5(29.9)	123.0(49.5)
$G_{LR}(R)$	42.8(18.5)	9.8(7.2)	—	19.8(9.9)	108.8(39.9)	123.0(60.3)
$G_{LR}(Y)$	31.5(11.8)	2.9(0.4)	12.7(7.6)	—	89.0(29.3)	118.5(48.9)
$G_{SM}(SM)$	23.6(10.1)	65.3(25.3)	75.1(32.4)	62.4(24.8)	—	29.5(18.9)
$G_{SM}(T_{3L})$	40.8(22.8)	84.8(39.7)	84.8(46.9)	81.8(39.3)	19.4(14.4)	—

A_{RFB}	SM	$G_{LR}(LR)$	$G_{LR}(R)$	$G_{LR}(Y)$	$G_{SM}(SM)$	$G_{SM}(T_{3L})$
SM	—	13.6(4.0)	19.0(7.2)	13.1(4.2)	7.8(2.7)	18.5(9.1)
$G_{LR}(LR)$	8.9(3.2)	—	6.4(3.2)	0.6(0.2)	6.9(1.4)	5.8(5.2)
$G_{LR}(R)$	12.6(5.6)	4.0(2.4)	—	7.1(3.0)	13.4(4.6)	0.6(2.0)
$G_{LR}(Y)$	8.6(3.4)	0.6(0.1)	4.8(2.3)	—	6.3(1.6)	6.4(5.0)
$G_{SM}(SM)$	5.0(2.1)	4.6(1.2)	8.9(3.6)	4.1(1.3)	—	12.7(6.6)
$G_{SM}(T_{3L})$	11.8(7.0)	3.3(3.8)	0.7(1.4)	4.0(3.7)	8.0(5.1)	—

Luminosity dependence

- Required integrated luminosity to achieve $s=3$ between models
 - Measure of the power of an asymmetry variable

$A_L \searrow A_{LL}$	SM	$E_6(\chi)$	$E_6(\eta)$	$E_6(\psi)$	$E_6(N)$	$E_6(S)$	$G_{LR}(B-L)$	$G_{LR}(LR)$	$G_{LR}(R)$	$G_{LR}(Y)$	$G_{SM}(SM)$	$G_{SM}(T_{3L})$
SM	–	62.6	5.1	10.6	38.7	>300	77.5	3.8	2.7	3.9	4.0	3.0
$E_6(\chi)$		–	10.2	32.7	>300	90.7	>300	7.1	4.6	7.5	7.7	5.2
$E_6(\eta)$			–	48.4	13.1	5.6	9.5	>300	45.3	>300	>300	70.7
$E_6(\psi)$				–	51.7	12.3	28.2	24.2	11.1	26.8	28.2	13.7
$E_6(N)$					–	51.6	>300	8.8	5.4	9.3	9.5	6.2
$E_6(S)$						–	117.8	4.2	3.0	4.3	4.4	3.3
$G_{LR}(B-L)$							–	6.6	4.3	6.9	7.1	4.9
$G_{LR}(LR)$	0.8							–	95.9	>300	>300	200.0
$G_{LR}(R)$	0.5							9.3	–	78.9	72.0	>300
$G_{LR}(Y)$	0.9							105.8	5.6	–	>300	151.7
$G_{SM}(SM)$	1.6							0.2	0.2	0.2	–	133.9
$G_{SM}(T_{3L})$	0.5							0.1	0.1	0.1	2.4	–

Spatial	SM	$G_{LR}(LR)$	$G_{LR}(R)$	$G_{LR}(Y)$	$G_{SM}(SM)$	$G_{SM}(T_{3L})$
SM	–	11.4(14.0)	5.6(6.6)	12.2(14.8)	35.7(42.6)	6.4(7.5)
$G_{LR}(LR)$	13.2(30.9)	–	55.0(59.1)	>300(>300)	42.6(55.1)	83.5(94.0)
$G_{LR}(R)$	7.1(14.3)	61.2(118.8)	–	38.7(51.7)	11.3(13.4)	>300(>300)
$G_{LR}(Y)$	13.7(33.0)	>300(>300)	55.3(98.4)	–	52.3(63.0)	56.1(79.6)
$G_{SM}(SM)$	40.0(97.6)	40.9(122.5)	11.8(28.9)	44.4(144.5)	–	14.0(16.6)
$G_{SM}(T_{3L})$	7.8(16.7)	94.0(204.9)	>300(>300)	82.8(161.5)	14.0(37.5)	–

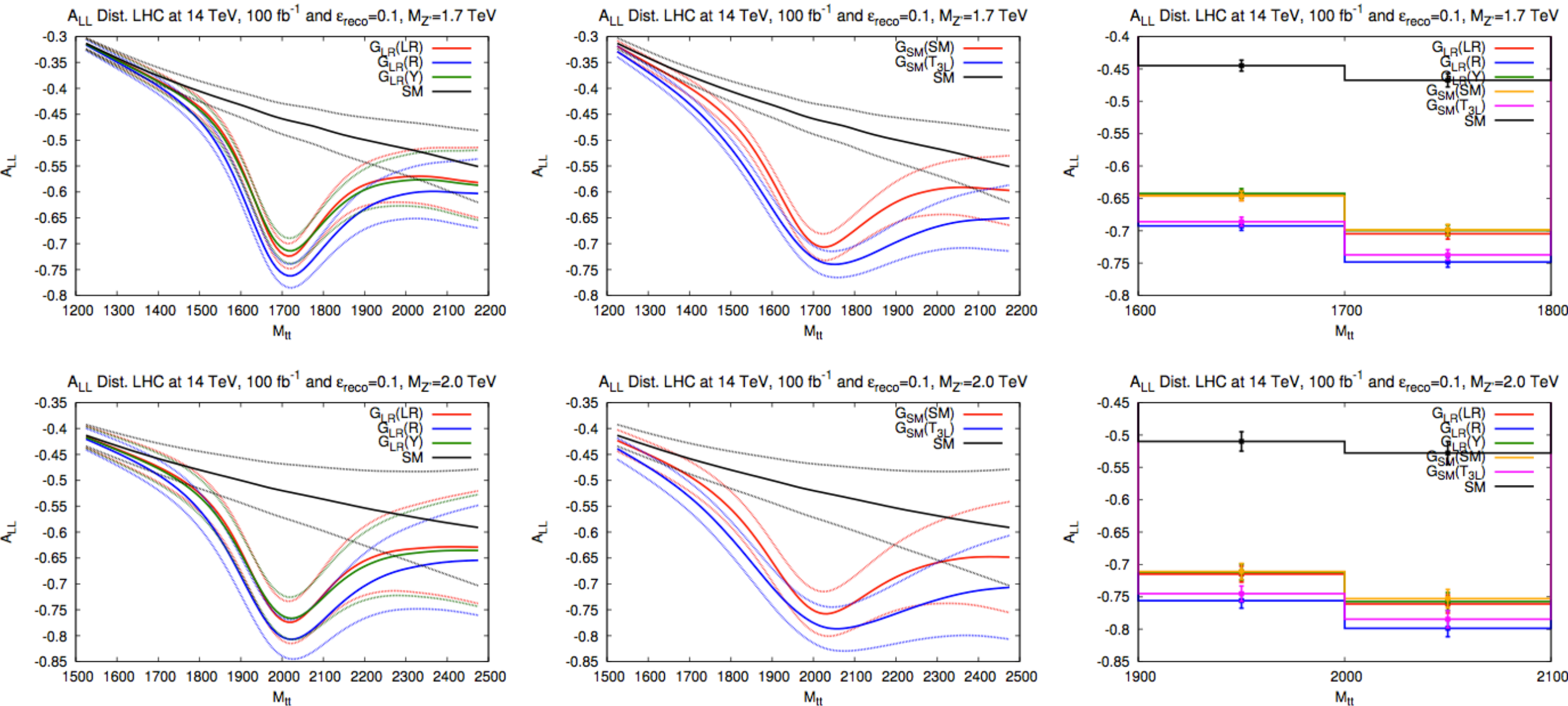
Conclusion

- Overview of a phenomenological study of spin and spatial asymmetries from a set of benchmark Z' models in $t\bar{t}b\bar{a}$ channel
- Quantified the ability to distinguish these models from the SM and among themselves
- Clear that the such models will be visible in the relatively early stages of LHC running ($<100 \text{ fb}^{-1}$)
- Spin asymmetries depend strongly on and are sensitive to the chiral couplings of the Z' and in some cases can disentangle models which would not be by cross section measurements

Outlook

- The set of benchmark models considered lend themselves to di-lepton searches
 - $t\bar{t}$ can compliment but not compete
- Other BSM scenarios with Z 's naturally have preferential couplings to the top or are leptophobic
 - Dynamical EWSB / composite Higgs
 - Extra dimensions
 - etc.
- Apply this kind of study to such models in which the $t\bar{t}$ channel is a competitive discovery mode

Generalised models: A_{LL}



- Larger couplings contribute to more visible effects, increased width
- Performs much worse than total cross section measurements
- Almost all models can clearly be discriminated from the SM but not between each other, G_{LR} and G_{SM} can be separated in the two bin plots

Generalised models: A_{LL}

- Some distinction is obtained in the integrated values from reduced statistical uncertainty and increased central values

$A_{LL}(\times 10)$	$\sqrt{s} = 14 \text{ TeV}$	$\mathcal{L}_{int} = 100 \text{ fb}^{-1}$	$\sqrt{s} = 8 \text{ TeV}$	$\mathcal{L}_{int} = 15 \text{ fb}^{-1}$
$M_{Z'} = 1.7 \text{ TeV}$	$\Delta M_{t\bar{t}} < 0.5 \text{ TeV}$	$\Delta M_{t\bar{t}} < 0.1 \text{ TeV}$	$\Delta M_{t\bar{t}} < 0.5 \text{ TeV}$	$\Delta M_{t\bar{t}} < 0.1 \text{ TeV}$
SM	-3.79 ± 0.05	-4.54 ± 0.07	-4.75 ± 0.39	-5.65 ± 0.61
$G_{LR}(LR)$	-4.41 ± 0.05	-6.72 ± 0.06	-5.48 ± 0.37	-8.03 ± 0.45
$G_{LR}(R)$	-4.70 ± 0.05	-7.18 ± 0.05	-5.83 ± 0.36	-8.38 ± 0.41
$G_{LR}(Y)$	-4.43 ± 0.05	-6.68 ± 0.05	-5.55 ± 0.37	-8.02 ± 0.44
$G_{SM}(SM)$	-4.52 ± 0.05	-6.69 ± 0.06	-5.64 ± 0.37	-8.04 ± 0.45
$G_{SM}(T_{3L})$	-4.94 ± 0.04	-7.09 ± 0.05	-6.12 ± 0.35	-8.31 ± 0.41
$M_{Z'} = 2.0 \text{ TeV}$	$\Delta M_{t\bar{t}} < 0.5 \text{ TeV}$	$\Delta M_{t\bar{t}} < 0.1 \text{ TeV}$	$\Delta M_{t\bar{t}} < 0.5 \text{ TeV}$	$\Delta M_{t\bar{t}} < 0.1 \text{ TeV}$
SM	-4.66 ± 0.09	-5.17 ± 0.11	-5.68 ± 0.84	-6.32 ± 1.23
$G_{LR}(LR)$	-5.41 ± 0.08	-7.36 ± 0.09	-6.53 ± 0.78	-8.51 ± 0.85
$G_{LR}(R)$	-5.74 ± 0.08	-7.75 ± 0.09	-6.90 ± 0.75	-8.79 ± 0.76
$G_{LR}(Y)$	-5.44 ± 0.08	-7.32 ± 0.09	-6.62 ± 0.77	-8.53 ± 0.82
$G_{SM}(SM)$	-5.53 ± 0.08	-7.30 ± 0.09	-6.69 ± 0.77	-8.51 ± 0.86
$G_{SM}(T_{3L})$	-5.99 ± 0.08	-7.63 ± 0.09	-7.16 ± 0.72	-8.72 ± 0.78